Computational Materials Science 50 (2011) 1811–1817

Contents lists available at ScienceDirect

Computational Materials Science

journal homepage: www.elsevier.com/locate/commatsci

Molecular dynamics simulations of dislocation interaction with voids in nickel

Aude Simar [a,b,*], Hyon-Jee Lee Voigt [a], Brian D. Wirth [a,c,1]

[a] Department of Nuclear Engineering, University of California, Berkeley, CA 94720-1730, USA
[b] Université catholique de Louvain, 1348 Louvain-la-Neuve, Belgium
[c] Department of Nuclear Engineering, University of Tennessee, Knoxville, TN 37996-2300, USA

ARTICLE INFO

Article history:
Received 13 December 2010
Received in revised form 10 January 2011
Accepted 13 January 2011

Keywords:
Molecular dynamics
Voids
Dislocations
Nickel
Dynamic effect

ABSTRACT

A high density of voids is expected to form in irradiated face centered cubic metals, which can have a negative impact on the ductility and cause an increasing strength. Molecular dynamics simulations of the interaction between gliding dissociated edge dislocations and voids in nickel have been performed to investigate the effect of the void size, the corresponding detachment mechanism, and dynamic effects of the dislocation on the obstacle strength. As expected, the void strength is observed to increase with increasing void size. The dislocation interaction and detachment process are determined by the applied shear stress, the repulsive interaction between partial dislocations and the image interaction between the partial dislocations and the void surface. For voids with a diameter smaller than 2 nm, the repulsive stress between the partials dominates, resulting in the detachment of the leading partial from the void while the trailing partial remains pinned. Consequently, the detachment process and obstacle strength are controlled by the trailing partial. For voids with a diameter larger than 2 nm, the attraction between the dissociated dislocations and the void dominates causing the detachment process and void strength to be influenced by both partials individually. This transition in detachment process at a void diameter of 2 nm is consistent with other research, and this transition is shown to be dependent on the void separation distance along the dislocation line and the dissociation distance between the partials, thus the stacking fault energy. Finally, by comparing the quasi-static and dynamic simulation results, an estimate for the static detachment stress is proposed in terms of the dynamic detachment stress and the dislocation velocity after detachment.

1. Introduction

Predicting the in-service performance of metals in fusion energy facilities is an inherently multiscale problem requiring both computational and experimental resources. High-energy neutron irradiation environments, in addition to α particles produced by fusion reactors, lead to the formation of high number density of nanometer-sized defect clusters, which can include dislocation loops, stacking fault tetrahedra (SFTs), defect clusters, nano-voids, and helium bubbles depending on the material and irradiation conditions [1]. Transmission electron microscopy (TEM) examinations demonstrate that faced centered cubic (FCC) metals with low to moderate stacking fault energy (e.g., gold and copper) tend to form SFTs [2]. Previously, molecular dynamics (MD) simulation methods have been successfully used in describing the complex interaction between moving dislocations and SFTs [3–5]. For FCC metals with moderate to large stacking fault energy (e.g., copper and nickel), the formation of nano-voids is frequently observed [2,6,7]. Many studies present models of the interaction of dislocations with those voids by either elasticity theory, molecular statics or molecular dynamics [8–14]. These results have shown that voids are strong obstacles by-passed with a similar stress to the one needed for the by-passing of impenetrable precipitates.

Our study focuses on the dislocation–void interaction in FCC nickel. Nickel and copper are model FCC metals for applications in nuclear reactors. Nickel has a larger stacking fault energy than the more studied copper, and hence the dissociation distance between Shockley partials is smaller. In FCC metals, the dislocation/void interaction is related to the behavior of Shockley partials and their interactions as part of the dislocation detachment process. Our paper addresses how Shockley partials affect the interaction behavior with voids by comparing with previous studies of dislocation/void interaction in copper [10,12]. A novel emphasis is also on the importance of dynamical effects, inherent to performing dislocation–obstacle interaction studies by using molecular dynamics simulations.

* Corresponding author at: Université catholique de Louvain, 1348 Louvain-la-Neuve, Belgium. Tel.: +32 10473565.
E-mail addresses: aude.simar@uclouvain.be (A. Simar), hyon-jee@nuc.berkeley.edu (Hyon-Jee Lee Voigt), bdwirth@utk.edu (B.D. Wirth).
[1] Tel.: +1 865 974 2525; fax: +1 865 974 0668.

0927-0256/$ - see front matter © 2011 Elsevier B.V. All rights reserved.
doi:10.1016/j.commatsci.2011.01.020

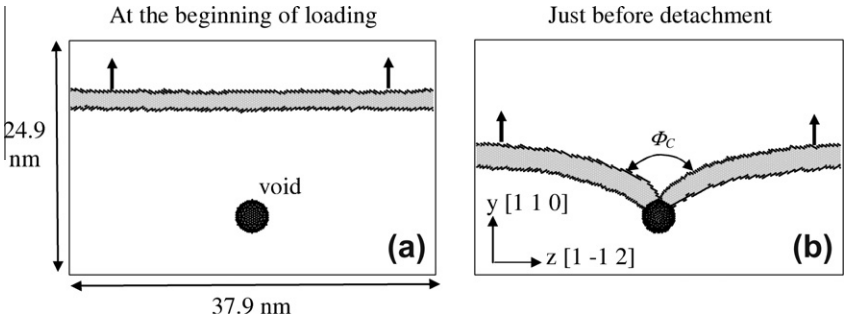

Fig. 1. Schematic of the molecular dynamics simulation box projected in the x direction. The perfect edge dislocation introduced in the simulation box dissociates into two Shockley partials (black lines) separated by a stacking fault (in grey) after 20 ps of relaxation time (a); when a shear stress is applied on the two free surfaces $x = \pm 9.2$ nm, the dislocation starts to glide until it gets pinned by the void (b). Φ_C is the detachment angle. The identification of the dislocation partials and of the stacking fault is based on a common neighbor analysis [18].

2. Description of the model

The molecular dynamics simulations are performed with the MDCASK code [15]. The FCC nickel embedded-atom potential of Mishin et al. [16] is used, and gives a stacking fault energy of 131 mJ/m^2 at 0 K which is close to the experimental range found by Carter and Holmes of 120–130 mJ/m^2 [17].

The simulations are performed with a constant temperature of 122 K. The simulation box has the following crystallographic orientation: x[−1 1 1], y[1 1 0] and z[1 −1 2], as shown in Fig. 1. An edge dislocation of infinite length in the z direction is introduced into the FCC lattice by removing two half (1 1 0) planes. Periodic boundary conditions are used in the y and z directions. In order to produce a shear stress that induces the dislocation movement, forces are applied in the y direction on the surface perpendicular to the x axis, following a relaxation at $T = 122$ K for 20 ps. These boundary conditions are similar to a study by Rodney and Martin [19]. The simulation box size is set to be $lx = 18.3$ nm, $ly = 24.9$ nm and $lz = 37.9$ nm. During the relaxation, the edge dislocation spontaneously dissociates into two Shockley partials separated by a stacking fault according to the reaction: $\frac{1}{2}[110] \rightarrow \frac{1}{6}[21\bar{1}] + \frac{1}{6}[121]$.

The shear stress is applied in two different manners:

- **Gradual increase of the applied shear stress (so called quasi-static simulations)**: The dislocation is allowed to intersect the void equator at a shear stress that is too low for the dislocation to by-pass the void. The stress is then gradually increased by steps of 5 MPa every 20 ps until the dislocation fully by-passes the void. In this case, the dislocation intersects the void with a low velocity. After the intersection, the segment of the dislocation in the vicinity of the void shows almost no mobility while the remainder of the dislocation line is kept at a low velocity due to the slow increase of the applied shear stress.
- **Constant applied shear stress (so called dynamical simulations)**: The dislocation is allowed to intersect the void equator at a shear stress that is sufficient for the dislocation to by-pass the void. In this case, the dislocation intersects the void with a high velocity.

The detachment angle of a Shockley dislocation partial (Φ_C) corresponds to the critical angle between the two branches of a partial dislocation right before escaping from the void. Fig. 1 presents the detachment angle of the leading partial. Since a precise extraction of Φ_C is not easy (with a precision of typically 10°), the comparison of detachment angles will be preferably made on the dislocation curvature in the vicinity of the void at detachment.

3. Results of the molecular dynamics simulations

3.1. Static and dynamic properties of the dislocation

The mean dissociation distance between the two Shockley partials (dd) without applied stress is equal to 2.72 nm with a standard deviation of 1 nm due to large fluctuations in their dissociation distance. The value of dd tends to increase if the box size is increased due to the periodicity of dislocations in the y direction (see also Rodney and Martin [20]). In a smaller simulation box ($ly = 14.9$ nm), the value of dd is slightly lower (2.53 ± 0.7 nm). These values of the dissociation distance are close to the experimental value of 2.6 ± 0.8 nm [17] and larger than the anisotropic elasticity result giving $dd = 1.82$ nm [17].

Table 1 gives dd and the steady-state velocity (v) of the edge dislocation as a function of the applied shear stress. The dislocation reached its steady-state velocity after gliding less than half of the simulation box. Increasing the applied shear stress increases the dislocation steady-state velocity [11,20] (Table 1). Rodney and Martin [20] reported a saturation of the dislocation velocity for an applied shear stress of 100 MPa. dd decreases with increasing applied shear stress (Table 1). The drag coefficient is given as $B = \tau b/v$ [21] here τ is the applied shear stress, b is the magnitude of the Burgers vector of the edge dislocation ($b = 0.249$ nm for an edge dislocation in nickel), and v is the dislocation velocity (v must be lower than half the sound wave velocity of the medium, i.e. 4970 m/s at 293 K for nickel). Based on a linear fit of the results presented in Table 1, the drag coefficient is estimated as 2.6×10^{-5} Pa s. This value is consistent with other values in the MD literature [11,19,20].

3.2. Void by-passing under a gradually increasing applied shear stress

When the applied shear stress is increased gradually (5 MPa every 20 ps) after the dislocation has been pinned by the void, the outer arms of the dislocation have a 20–100 times lower velocity than the steady-state velocity at the same applied shear stress level. The velocities of these arms during a gradual increase of the applied shear stress is about 10 m/s.[2]

Fig. 2 compares the shapes of the dislocation branches at detachment for the leading and the trailing partials when the applied shear stress is gradually increased. First, it can be observed that the shape at detachment is asymmetrical due to the mixed character of the Shockley partials. This asymmetry is opposite for the leading partial and the trailing partial since their Burgers vec-

[2] This velocity corresponds to a shear strain rate of about $\dot{\varepsilon} = 5.5 \times 10^6$ s^{-1} based on the Orowan relation $\dot{\varepsilon} = \rho_m b v$ (where ρ_m is the density of mobile dislocations).

Table 1
Edge dislocation dissociation distance and steady-state velocity as a function of the applied shear stress (box size: $lx = 18.3$ nm, $ly = 24.9$ nm and $lz = 37.9$ nm).

Applied shear stress τ (MPa)	Dissociation distance dd (nm)	Steady-state velocity v (ms^{-1})
0	2.72 ± 1.00	0
10	2.55 ± 0.73	243
75	2.42 ± 0.53	786
150	2.25 ± 0.44	1303

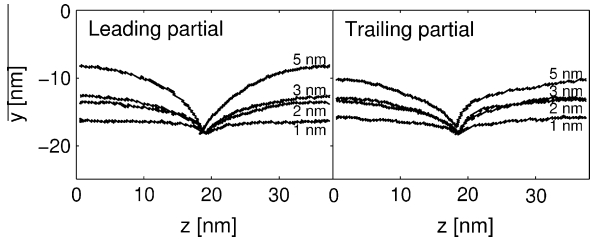

Fig. 2. Effect of the void size on the shape of the leading and trailing partials at detachment when the applied shear stress is gradually increased by 5 MPa every 20 ps. The dislocation lines are shifted in the y direction by the void radius to allow an easy comparison.

tors are oriented respectively at +30° and −30° to the Burgers vector of the un-dissociated dislocation. Fig. 2 shows that the detachment angle of the leading and the trailing partial decreases with increasing void size.

Fig. 3 shows that the applied shear stress needed for a dislocation detachment increases as the void diameter increases. The stress required for a tailing partial to detach is larger than that of the leading partial for the 1 nm void, while the other voids simulated required the same level of stress for the detachment of each partial dislocation. For the 1 nm void, the sequences leading to the dislocation detachment are presented in Fig. 4. At the applied shear stress of 5 MPa (Fig. 4, $t = 145$ ps), both partials are pinned by the void initially, but the trailing partial is repelled away from the void after 40 ps. The trailing partial stays at a stable separation distance away from the leading partial, which remains pinned by the void (Fig. 4, $t = 190$ ps). After the stress is increased to 25 MPa (Fig. 4, $t = 270$ ps), the trailing partial glides forward and enters the void, while the leading partial is still unable to detach from the void.

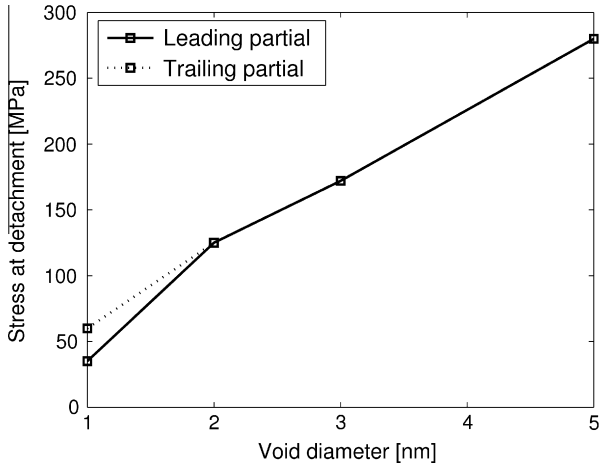

Fig. 3. The applied shear stress at the time of detachment as a function of the void diameter when the applied shear stress is gradually increased by 5 MPa every 20 ps (i.e. quasi-static condition).

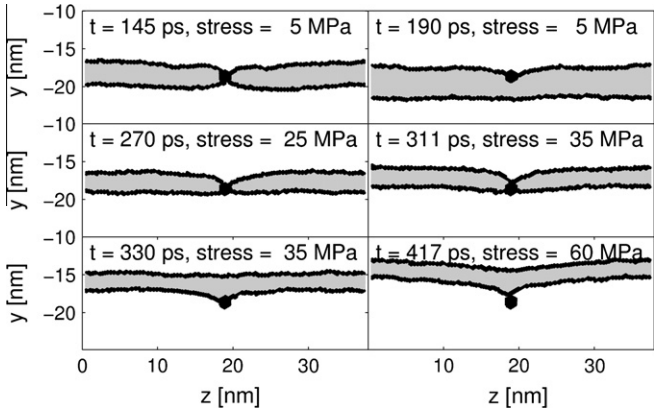

Fig. 4. Evolution of the dislocation shape when interacting with a 1 nm void when the applied shear stress is gradually increased by 5 MPa every 20 ps (i.e. quasi-static condition).

This causes a local repulsion of the partials in the vicinity of the void. Both the leading and trailing partials remain pinned by the void until the detachment of the leading partial occurs at the applied shear stress of 35 MPa (Fig. 4, $t = 311 - 330$ ps). The trailing partial remains pinned by the void until the stress is increased to 60 MPa (Fig. 4, $t = 417$ ps). However, for 2 nm voids and larger, the trailing partial detaches at the same stress level as the leading partial. The change of detachment behavior as a function of void size is discussed in Section 4.

3.3. Void by-passing with a constant applied shear stress

Table 2 presents the applied shear stresses required for the leading and trailing partials to detach from a void as a function of the void diameter. Independent of the void diameter, a larger applied shear stress is necessary for the trailing partial to detach

Table 2
Stress needed for the detachment of the leading and trailing partial when the applied shear stress is maintained constant during the entire simulation (i.e. dynamic simulation). Velocities of the dislocation when entering the void and when leaving the void for the applied stress mentioned in the third column.

Void diameter (nm)	Applied stress for only the leading partial to detach (MPa)	Applied stress for the trailing partial to detach (MPa)	Velocity before the leading partial enters the void (m/s)	Velocity after the trailing partial leaves the void (m/s)
1	10	40	584	251
2	unavailable	75	774	459
3	75	110	932	725
5	>160	180	1567	990

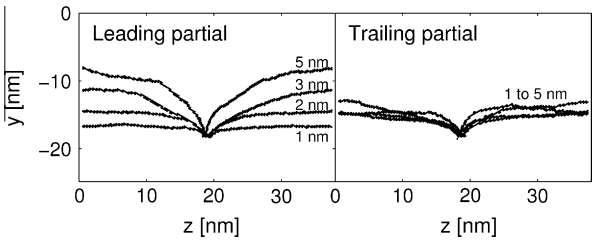

Fig. 5. Effect of the void size on the shape of the leading and trailing partials at the time of detachment when the applied shear stress is kept constant at 40 MPa for the 1 nm void, 75 MPa for the 2 nm void, 110 MPa for the 3 nm void, and 180 MPa for the 5 nm void (i.e. dynamic condition). The dislocation lines are shifted by the void radius to allow an easy comparison.

Table 3
Comparison between the various simulations in the literature and in the present study concerning the transition diameter D_{trans}.

	Material	Equilibrium dissociation distance *dd* (nm)	Box size in z direction (nm)	Strain rate, $\dot{\varepsilon}$ (s^{-1})	Temperature (K)	Velocity (m/s)	Transition void diameter, D_{trans} (nm)
Hatano and Matsui [10]	Cu	4	23	10^6	300	NA	<0.6
Osetsky and Bacon [12,14]	Cu	4	35.5	5×10^6	0	20	~2.5
Present study	Ni	2.7	37.9	$\sim 5.5 \times 10^6$	122	10	1–2

from the void compared to the leading partial. Fig. 5 shows the shape of the leading and the trailing partials at detachment. As the void diameter increases from 1 nm to 5 nm, the bowing of the leading partial increases, thus the detachment angle decreases. Contrary to the behavior observed for the detachment of the leading partial, the trailing partial does not show prominent bowing with increasing void diameter.

4. Discussions about the molecular dynamics simulations

Dislocation–void interactions in Ni involve highly correlated physical processes that have several implications on scales far beyond those covered by MD. Geometric aspects of the simulations impose physical characteristics of the material in the global sense. For example, the length of the MD simulation box along the dislocation line prescribes the average void density and inter-obstacle spacing, while the two dimensions perpendicular to it affect the dislocation density and thus the strain rate calculated from the Orowan relation. The void size determines the detachment angle, which inturn establishes the degree of hardening in the material. Physical aspects of the simulations, such as the imposed boundary conditions (applied stress, temperature, etc.), govern the dynamics of the dislocation, which establishes how meaningful a comparison can be made with experiments and other theories. For example, the fashion in which external tractions are applied, in conjunction with other geometric aspects just mentioned, determines the dynamic behavior of the dislocations. This feeds back into the calculated strengthening due to void formation because it determines how the energy supplied to the system is expended. The chosen temperature affects the strain rate (through viscous damping processes that limit the dislocation velocity) and how the mechanical heat is dissipated in the system. Finally, numerical aspects, such as the integrator chosen and the time step used determine the stability and time scale of the simulations, respectively.

MD is subject to a number of limitations that restrict what can be simulated. However, understanding these aspects and their effects are crucial to determine the applicability of this methodology and the value in context with the very real problem of predicting the mechanical behavior in irradiated materials. Below we touch on several important aspects of the simulations and their implications vis-à-vis the overall mechanical behavior of the material and the meaningfulness of the comparison with experimental measurements.

4.1. Effect of the void size

The molecular dynamics simulations, performed under conditions of a gradually increasing applied shear stress, or at a constant applied shear stress, have shown that the critical resolved shear stress for a dislocation to by-pass voids increases with increasing void diameter (Fig. 3 and Table 2). Note that the box size in these simulations was kept constant, hence the inter-obstacle spacing between voids is slightly decreased as the void size is increased. This is expected to have a second order effect on the strengthening. Scattergood and Bacon [9] found the same void size effect by a discrete dislocation model based on a simple assumption of the dislocation/void interaction. Osetsky and Bacon [12,14] and Hatano and Matsui [10] present similar results for molecular dynamics simulations of the dislocation/void interaction in copper. The detachment angle decreases with void size (see Fig. 2). The decrease of the detachment angle corresponds with an increase of the obstacle strength based on the line tension model [22]. The obstacle strength increase with void size is attributed to the increasing contact length between the dislocation and the void associated with the local annihilation and re-nucleation of a larger dislocation segment for a larger void.

4.2. Detachment of the leading and the trailing partial

The evolution of the detachment stress with void diameter in the case of a gradually increasing applied shear stress (see Fig. 3) demonstrates that the trailing partial determines the resistance of the void against the edge dislocation glide for small voids, while both partials determine the resistance of the void against the edge dislocation glide for larger voids (typically of a diameter larger than 2 nm). The parameter D_{trans} is defined as this transition void diameter; here D_{trans} is 1–2 nm.

A possible reason for this transition is discussed using the detachment mechanism observed for the 1 nm void (Fig. 4). After the applied shear stress has reached 25 MPa, the pinning of both partial dislocations leads to a strong local repulsion since the partials remain closer than their equilibrium dissociation distance in the vicinity of the void. This configuration results from the balance between the applied shear stress and the energy associated with the dislocation line in the vicinity of the void and the stacking fault area. Away from the void pinning site, the partial dislocations are at their stable dissociation distance, i.e. typically 2.4 nm for an applied shear stress equal to 25–35 MPa (Table 1). When the applied shear stress is increased above 35 MPa, the configuration in which the leading partial remains attached to the void becomes unstable hence the leading partial detaches and glides away from the void. Subsequently, the equilibrium dissociation distance between the leading and trailing partial dislocations is restored in the vicinity of the void. However, for a void diameter of 2 nm and larger, the stable dissociation distance is close to or smaller than the void diameter. In this case, the repulsion of the partials in the void vicinity is not strong enough to assist the detachment of the leading partial. Thus, both partials detach at the same level of applied shear stress.

Table 3 compares the conditions and results of the study by Osetsky and Bacon [12,14], Hatano and Matsui [10], and the present study concerning the transition between the trailing partial dominated detachment process and when both partials determine the detachment process. Table 3 shows that D_{trans} increases as the equilibrium dissociation distance (*dd*) and/or the void spacing along the dislocation line increases when the strain rate[3] and the temperature[4] effect on D_{trans} are ignored.

[3] Osetsky and Bacon [14] have found no influence of the strain rate on the critical stress for large void (6 nm in diameter) by-passing for strain rates between 5×10^6 s^{-1} and 10^7 s^{-1}

[4] Above 100 K, no influence of the temperature on the critical stress at detachment is observed for voids of sizes typical of Dtrans [10,12,14].

When the void spacing is comparable, D_{trans} is larger for Cu ($D_{trans} \sim 2.5$ nm) than for Ni ($D_{trans} \sim 1$–2 nm) due to the larger *dd* of Cu. The larger *dd* implies that the leading partial prefers to stay further away from the trailing partial, making the effective repulsion between the leading and the trailing partial stronger when they are pinned together by a small void. Thus, a stronger repulsion, enough to induce an expulsion of the leading partial, can be achieved when *dd* is larger for the same void size. This effectively increases the D_{trans} as *dd* increases.

When *dd* is comparable as in the two Cu cases, D_{trans} is found to be smaller for a smaller void spacing (Table 3). For example, D_{trans} is decreased from 2.5 nm to a lower value than 0.6 nm when the void spacing is decreased from 35.5 nm to 23 nm. The most noticeable effect of void spacing decrease is an increase of the detachment stress. For a 2 nm diameter void at 300 K in Cu, Hatano and Matsui [10] (a void spacing of 23 nm) obtain a critical stress for dislocation detachment about 1.5 times larger than that of Osetsky and Bacon [14] (a void spacing of 35.5 nm). Thus, it is reasonable to think that the stress required for a leading partial to detach from a void also increases with decreasing void spacing. As a consequence, the expulsion of the leading partial from the void due to the repulsion from the trailing partial can only occur when the void diameter is much smaller, i.e. when the dislocation partials are forced to remain significantly closer than their equilibrium distance, otherwise the two partials will remain pinned by the void. Hence, the transition from trailing partial dominated detachment process to both partials dominated process will occur only at a smaller void size when the void spacing is decreased. Effectively, this results in the decrease of D_{trans} as the void spacing decreases.

4.3. Generality of the detachment angle

Figs. 6 and 7 compare the shapes of the partial dislocation lines at the time of detachment from the void as a function of the applied stress changing from gradually increasing to constantly applied shear stress. The angle at detachment is essentially the same, whether the applied stress is constant or gradually increased, even though the dislocation velocities and the stresses at detachment are very different. Hence, the detachment angle is found to be weakly dependent on the velocity of the partials at detachment. This finding can be explained using the dislocation behavior at the moment of detachment. When detachment is about to occur, the dislocations on each side of the void become close enough for the interaction between the dislocations of opposite sign to dominate. Hence, the local shape of the dislocation around the void

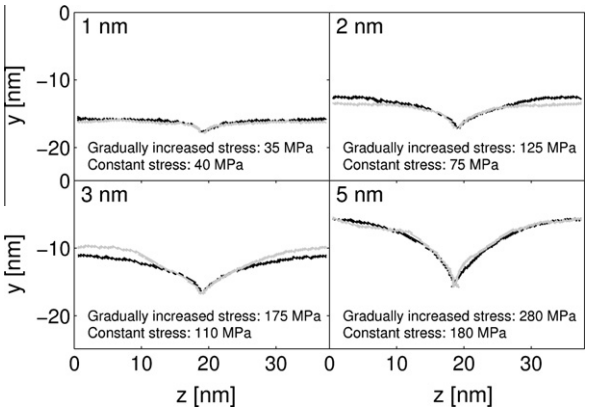

Fig. 6. Comparison of the shape of the leading partial at detachment for various void diameters when the applied shear stress is either gradually increased (i.e. quasi-static condition) or constant (i.e. dynamic condition) at the specified value.

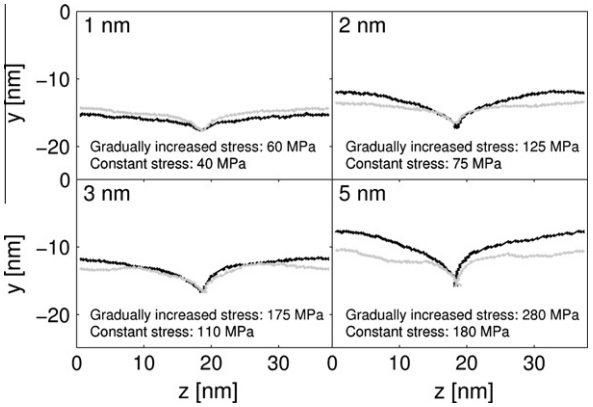

Fig. 7. Comparison of the shape of the trailing partial at detachment for various void diameters when the applied shear stress is either gradually increased (i.e. quasi-static condition) or constant (i.e. dynamic condition) at the specified value.

at detachment is independent of velocity and thus it is not significantly influenced by the artificially large strain rates involved in MD simulations. Furthermore, MD simulations offer the advantage of taking the dislocation core structure into account which is of great importance in the dislocation/void interaction.

4.4. Dynamic effects

However, dynamic effects do have a prominent affect on the behavior of the dislocation/void interaction. The shear stress at which the dislocation by-passes a void is always larger when the shear stress is gradually increased, typically by a factor of 1.5 compared to the value needed for detachment at a constant applied stress condition (comparing Fig. 3 to Table 2). Under a constant applied shear stress of 10 MPa, the dislocation velocity when intersecting the void is 20 times the dislocation velocity when a gradually increased shear stress is applied (see Table 1 and Section 3.2). A large dislocation velocity favors the void by-passing owing to the dynamics of the dislocation.

The literature provides similar evidences of strong dynamic effects on the dislocation/obstacle interaction at very high dislocation velocities. Bitzek and Gumbsch [11] performed simulations of the by-passing of a 1 nm void by an edge dislocation in nickel (voids spacing is 30 nm). This void is by-passed under a static stress (corresponding to the gradually increased applied shear stress) equal to 55 MPa, while it was 18 MPa when the stress was applied dynamically (corresponding to the constant applied shear stress). Fusenig and Nembach [23] have experimentally measured the critical resolved shear stress for the detachment of dislocations in copper single crystals from cobalt-rich precipitates and also concluded for the existence of strong dynamic effects. As observed in the present study, they found that damping of the dislocation motion is so low at temperatures below 200 K that dislocations acquire kinetic energy while gliding in between the precipitates helping the dislocations to overcome them.

Table 2 shows that only the leading partial is able to detach from a 3 nm void at a constant applied shear stress of 75 MPa. When a constant stress of 110 MPa is applied, both partials are able to detach from the void. However, Fig. 3 shows that both partials determine the strength of the 3 nm void against the dislocation by-passing when the stress is gradually increased. This difference arises from the dynamic effect that affects the individual dislocation interaction behavior with voids. For the 3 nm void at an applied shear stress of 75 MPa, the leading partial has enough kinetic energy to compensate the attraction from the void but

the dislocation is slowed down by the pinning and the detachment process. Hence the trailing partial has not sufficient kinetic energy to by-pass the void along with the leading partial. For a constant applied shear stress of 110 MPa, the remaining kinetic energy after the by-pass of the leading partial is sufficient for the trailing partial to also detach from the void. The trailing partial detaches with the same angle Φ_C as in the simulations where the stress is gradually increased (see Fig. 7 and Section 4.3.).

When the applied stress is constant, Fig. 5 shows that the void size has little influence on the bowing of the trailing partial at detachment. This is due to the dynamic effects of dislocation and void interactions. After interacting with the void, the leading partial is slowed down (Table 2) but continues to glide and drag the trailing partial. Hence, the position of the trailing partial is mainly a function of the velocity of the leading partial except for the part that interacts with the void.

The equation of motion of a dislocation is invoked to further understand the dynamics of the dislocation. The local balance of stresses at an obstacle can be expressed as [21]:

$$\tau_{ext} + \tau_{obs} = \tau_{back} + \tau_{drag} + \tau_{inertia} \quad (1)$$

where τ_{ext} is the applied resolved shear stress, τ_{obs} is the obstacle strength (here the void), τ_{back} is the resistance associated with the line tension, $\tau_{drag} = Bv/b$ is the viscous drag (B is the drag coefficient) and $\tau_{inertia}$ is the contribution from inertial effects associated to accelerations and decelerations of the dislocation. The last term, $\tau_{inertia}$ is proportional to the variation in velocity with time [21]:

$$\tau_{inertia} = \frac{m}{b}\frac{\partial v}{\partial t} \quad (2)$$

where m is the effective mass of the dislocation. Bitzek and Gumbsch [11] evaluate m as equal to 1.5×10^{-16} Ns^2/m^2. The deceleration of the dislocation when crossing the void can be estimated by the time needed to decelerate the dislocation passing by the 3 nm void, which is about 15 ps. This dislocation intersects the void at a velocity of 932 m/s and leaves it at a velocity of 725 m/s (see Table 2). This corresponds to a deceleration of 1.4×10^{13} m/s^2. Neglecting the effect of velocity on the effective mass, Eq. (2) gives $\tau_{inertia}$ = 8 MPa which can be considered as a second order contribution compared to the associated τ_{drag} equal to 76 MPa. Note that $\tau_{inertia}$ is not as negligible for a 1 nm void for which it is about 50% of τ_{drag}.

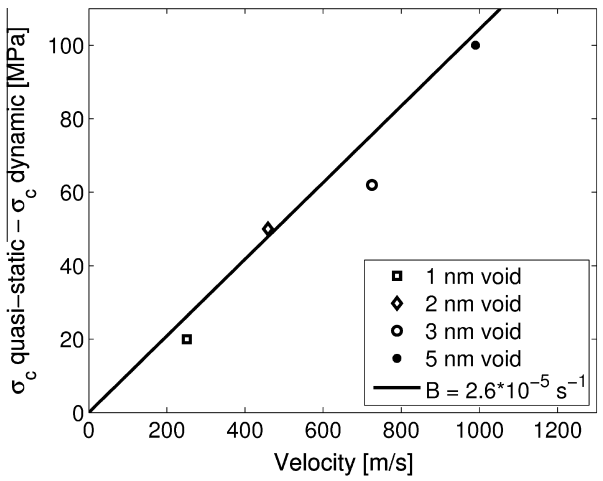

Fig. 8. Difference between the quasi-static stress at detachment for the trailing partial (Fig. 3) and the constant stress allowing the full dislocation to detach the void (Table 2) as a function of the velocity of the dislocation when leaving the void. The solid line is for σ_C(quasi-static)–σ_C(dynamic) = B/bv (B is the drag coefficient equal to 2.6×10^{-5} Pa s, see Section 3.1).

The gradually increased applied shear stress simulations are performed at a very small velocity compared to the velocity of the dislocation in the constant applied stress simulations. Hence we can consider that both τ_{drag} (~2 MPa) and $\tau_{inertia}$ are negligible in these simulations. Hence, by subtracting the "dynamic" stress (i.e. constant applied shear stress) at detachment from the "quasi-static" stress (i.e. gradually increased applied shear stress) at detachment should give $\tau_{drag} + \tau_{inertia}$. This assumes that τ_{back} is independent of the dislocation velocity at detachment, but since the detachment angles are similar for the dynamic and static simulations, this may be a valid approximation. If $\tau_{inertia}$ is neglected, it is expected that the dynamic term scales with the velocity with a slope equal to B/b. Fig. 8 shows the difference between the "quasi-static" stress at detachment and the "dynamic" stress at detachment as a function of the velocity of the dislocation when leaving the void. A good correlation is obtained. Fig. 8 offers a way of obtaining static detachment stresses, or obstacle strengths, from dynamic simulations.

5. Conclusions

Molecular dynamics simulations of the interaction between dissociated edge dislocations and voids have been performed in nickel. The following conclusions can be drawn:

- The obstacle strength of voids increases with void size, due to the increasing contact length between the dislocation and the void.
- The leading partial detaches at a smaller applied shear stress for a void 1 nm in diameter, while the leading and trailing partial detach at the same applied shear stress from voids of 2 nm in diameter and larger. This is likely the result of the elastic interaction between Shockley partials of a dissociated perfect dislocation in the vicinity of the void. For a 1 nm void, the partials pinned by the void strongly repel in the vicinity of the void assisting the detachment of the leading partial. The trailing partial detaches at a higher applied stress. For voids of 2 nm and larger, the repulsion between partials are not strong enough to favor the detachment of either partials, thus they detach at the same applied stress.
- The detachment angles are similar, irrespective of the manner the shear stress is applied, (constant vs. gradually increasing) providing the perspectives to analyze dislocation/obstacle interactions by dynamic simulations.
- Strong dynamic effects influence the stress level at which the void is by-passed by a dislocation. This dynamic stress can be estimated in dynamic simulations using the dislocation velocity when leaving the obstacle and the drag coefficient of the material at the working temperature. This estimation has been shown to successfully reproduce the difference in detachment stress between quasi-static simulations and the dynamic simulations.

Acknowledgements

A. Simar is a Postdoctoral Researcher of the FNRS-FRS (Belgium). The calculations have partly been performed on the CISM-UCL, Belgium computer facilities. The authors acknowledge the comments of Yves Bréchet (INP, Grenoble), Jaime Marian (LLNL) and Thomas Pardoen (UCL, Belgium). The authors gratefully acknowledge financial support at UCB from the National Science Foundation under contract NSF DMR 0244562 and the Department of Energy, Office of Fusion Energy Sciences under grant DE-FG02-04GR54750.

References

[1] G. Was, Fundamentals of Radiation Materials Science. Metals and alloys, Springer, Berlin, 2007.
[2] S.J. Zinkle, L.L. Snead, J. Nucl. Mater. 225 (1995) 123–131.
[3] B.D. Wirth, V. Bulatov, T. Diaz de la Rubia, J. Nucl. Mater. 283–287 (2000) 773–777.
[4] Y.N. Osetsky, R.E. Stoller, D. Rodney, D.J. Bacon, Mater. Sci. Eng. A 400–401 (2005) 370–373.
[5] L. Saintoyant, H.-J. Lee, B.D. Wirth, J. Nucl. Mater. 361 (2007) 206–217.
[6] J.L. Brimhall, B. Mastel, J. Nucl. Mater. 33 (2) (1969) 186–194.
[7] V.I. Dubinko, A.G. Guglya, E. Melnichenko, R. Vasilenko, J. Nucl. Mater. 385 (2) (2009) 228–230.
[8] J.R. Willis, M.R. Hays, R. Bullough, Proc. R. Soc. Lond. A329 (1972) 121–136.
[9] R.O. Scattergood, D.J. Bacon, Acta Met. 30 (1982) 1665–1677.
[10] T. Hatano, H. Matsui, Phys. Rev. B 72 (2005) 094105.
[11] E. Bitzek, P. Gumbsch, Mater. Sci. Eng. A 400–401 (2005) 40–44.
[12] Y.N. Osetsky, D.J. Bacon, Mater. Sci. Eng. A 400–401 (2005) 374–377.
[13] H.-J. Lee, B.D. Wirth, J. Nucl. Mater. 386–388 (2009) 115–118.
[14] Y.N. Osetsky, D.J. Bacon, Philos. Mag. 90 (7–8) (2010) 945–961.
[15] T. Diaz de la Rubia, M.W. Guinan, J. Nucl. Mater. 174 (2–3) (1990) 151–157.
[16] Y. Mishin, D. Farkas, M.J. Mehl MJ, D.A. Papaconstantopoulos, Phys. Rev. B 59 (5) (1999) 3393–3402.
[17] C.B. Carter, S.M. Holmes, Philos. Mag. 35 (1977) 1161–1172.
[18] A.S. Clarke, H. Jonsson, Phys. Rev. E 47 (1993) 3975–3985.
[19] D. Rodney, G. Martin, Phys. Rev. Lett. 82 (16) (1999) 3272–3275.
[20] D. Rodney, G. Martin, Phys. Rev. B 61 (13) (2000) 8714–8725.
[21] E. Nembach, Particle Strengthening of Metals and Alloys, Wiley J and Sons, New York, 1996.
[22] J.W. Martin, Micromechanisms in Particle-Hardened Alloys, Cambridge University Press, Cambridge, UK, 1980.
[23] K.-D. Fusenig, E. Nembach, Acta Metall. Mater. 41 (1993) 3181–3189.